Inorganic Chemistry

Article

pubs.acs.org/IC

Multinuclear Copper(I) Guanidinate Complexes

Alexander M. Willcocks,[†] Thomas P. Robinson,[†] Christopher Roche,[†] Thomas Pugh,[†] Stephen P. Richards,[†,‡] Andrew J. Kingsley,[‡] John P. Lowe,[†] and Andrew L. Johnson*[,†]

[†]Department of Chemistry, University of Bath, Bath, BA2 7AY, United Kingdom

[‡]SAFC-Hitech, Power Road, Bromborough, Wirral, CH62 3QF, United Kingdom

Supporting Information

ABSTRACT: A series of multinuclear Copper(I) guanidinate complexes have been synthesized in a succession of reactions between CuCl and the lithium guanidinate systems Li{**L**} (**L** = $Me_2NC(^iPrN)_2$ (**1a**), $Me_2NC(CyN)_2$ (**1b**), $Me_2NC(^tBuN)_2$ (**1c**), and $Me_2NC(DipN)_2$ (**2d**) (^{i}Pr = iso-propyl, Cy = cyclohexyl, ^{t}Bu = *tert*-butyl, and Dip = 2,6-*di*isopropylphenyl) made in situ, and structurally characterized. The *di*-copper guanidinates systems with the general formula $[Cu_2\{L\}_2]$ (**L** = $\{Me_2NC(^iPrN)_2\}$ (**2a**), $\{Me_2NC(CyN)_2\}$ (**2b**), and $\{Me_2NC(DipN)_2\}$ (**2d**) differed significantly from related amidinate complexes because of a large torsion of the dimer ring, which in turn is a result of transannular repulsion between adjacent guanidinate substituents. Attempts to synthesis the *tert*-butyl derivative $[Cu_2\{Me_2NC(^tBuN)_2\}_2]$ result in the separate formation and isolation of the *tri*-copper complexes $[Cu_3\{Me_2NC(^tBuN)_2\}_2(\mu\text{-}NMe_2)]$ (**3c**) and $[Cu_3\{Me_2NC(^tBuN)_2\}_2(\mu\text{-}Cl)]$ (**4c**), both of which have been unambiguously characterized by single crystal X-ray diffraction. Closer inspection of the solution state behavior of the lithium salt **1c** reveals a previously unobserved equilibrium between **1c** and its starting materials, $LiNMe_2$ and *N,N′*-di-*tert*-butyl-carbodiimide, for which activation enthalpy and entropy values of $\Delta H^{\ddagger} = 48.2 \pm 18$ kJ mol^{-1} and $\Delta S^{\ddagger} = 70.6 \pm 6$ J/K mol have been calculated using 1D-EXSY NMR spectroscopy to establish temperature dependent rates of exchange between the species in solution. The molecular structures of the lithium complexes **1c** and **1d** have also been determined and shown to form tetrameric and dimeric complexes respectively held together by Li−N and agostic Li···H−C interactions. The thermal chemistry of the copper complexes have also been assessed by thermogravimetric analysis.

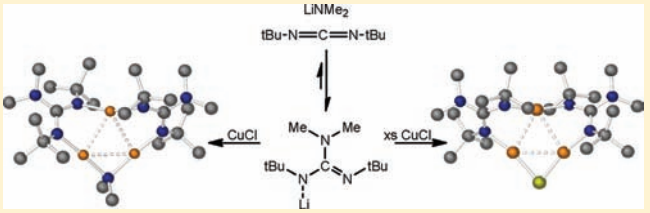

INTRODUCTION

Anionic bridging ligands such as guanidinates, amidinates, and triazenides (Chart 1) continue to evolve as versatile *N,N′*-donor ligands in coordination chemistry largely because of the range of derivatives available through substitution at the terminal nitrogen atoms, and are capable of imparting a significant degree of electronic and steric stabilization.[1]

Amidinate, guanidinate, and triazenide ligands have been widely used with Group 11 metals to form a range of multinuclear complexes,[2] with varying coordination arrangements, which typically support Cu(I)−Cu(I), Ag(I)−Ag(I), and Au(I)−Au(I) interactions between formally closed shell metal centers (d^{10}-d^{10}).[3] Such complexes have been the subject of considerable attention for some time, specifically with respect to the ability to control such metallophilic bonding.[2h,j,4] More recently these systems have attracted attention as potential metal deposition precursors,[2d−g,l,5] catalysts[6] and as model systems for the study of spin delocalization superexchange pathways.[2b,c]

The guanidinate ligand systems have available to them a zwitterionic iminium/diamide type resonance structure, arising from the delocalization of the lone pair on the uncoordinated nitrogen into the $\{CN_2\}$ component of the ligand (Chart 1). This delocalization results in an imposed coplanarity of the $\{NR_2\}$ and $\{CN_2\}$ components of the ligand, which can result in significant steric repulsion between the nitrogen substituents, and can have an effect on the projection of the two *N*-donor

Chart 1. General Formulae of the Amidinate, Guanidinate and Triazenide Anions, and the Resonance Forms of the 1,2,2,3-Tetra-alkyl Guanidinate Ligand[a]

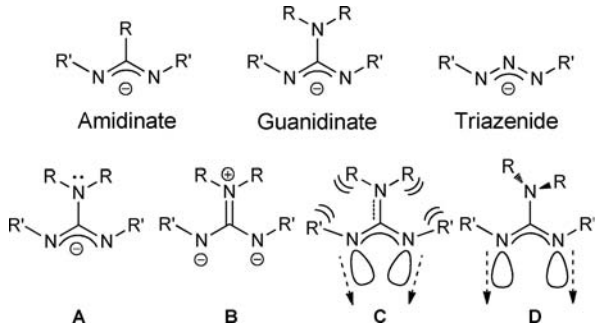

[a](**A**) 1,3-diazaallyl resonance form, (**B**) the iminium/diamide resonance form, and (**C** and **D**) the effect of π-delocalization on the steric interactions and *N*-orbital projections in the ligand.

Received: July 26, 2011
Published: December 14, 2011

Chart 2. General Formulae of the Three Distinct Classes of Guanidinate Anion (m/n = 0 or 1)

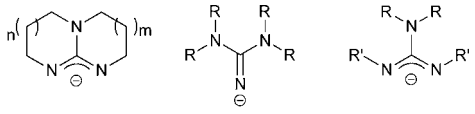

atom orbitals. Rotation about the C−NR_2 bond, such that the {NR_2} substituent is no longer coplanar with the {CN_2} component alleviates both steric repulsion and constriction of the ligands bite-angle, but with the loss of delocalization over the {CN_3} backbone.

This central {CN_3} core unit, derived from the biologically important guanidine molecule, [$HN{=}C(NH_2)_2$],[7] is present in three distinct classes of guanidinate ligand; specifically bicyclic guanidinate systems,[8] 1,1,3,3-tetra-alkyl guanidinate systems,[2i,9] and 1,2,2,3-tetra-alkyl guanidinate systems,[2g,5] all three of which have been exploited in the coordination chemistry of Group 11 metals. (Chart 2).

Copper(I) amidinate dimers have been reported as potential chemical vapor deposition (CVD) and atomic layer deposition (ALD) precursors,[2d,e] and more recently Barry and co-workers have described the synthesis, molecular structure, and gas phase thermolysis of the copper(I) guanidinate complexes [$Me_2NC(^iPrN)_2Cu]_2$ and [$^iPrN(H)C(^iPrN)_2Cu]_2$.[2g,5]

In this report, we expand this family of complexes and describe the synthesis and characterization of a series of multinuclear copper complexes bearing 1,2,2,3-tetra-alkyl/aryl guanidinate ligands of the general formula {$(NR)_2CNMe_2$} where R = ^{i}Pr, Cy, ^{t}Bu and 2,6-*di*isopropylphenyl. These compounds were characterized by single-crystal X-ray diffraction. In all cases complexes ^{1}H and ^{13}C NMR studies and microanalysis were consistent with the formulation derived from single crystal data.

RESULTS AND DISCUSSION

Synthesis and Characterization. Inspired by the work of Gordon et al.,[10−15] our initial interest was to synthesize a range of guanidinate complexes and assess the effect of varying the substituents on the nitrogen atoms of the {CN_2} unit, on the precursors suitability toward copper ALD and CVD.

The *di*-copper(I) guanidinates [{$Me_2NC(^iPrN)_2$}$_2Cu_2$], [{$Me_2NC(CyN)_2$}$_2Cu_2$], [{$Me_2NC(^tBuN)_2$}$_2Cu_2$], and [{$Me_2NC(DippN)_2$}$_2Cu_2$] (Dip = 2,6-disopropylphenyl) were identified as the initial target complexes, and their synthesis was attempted following a modification of the literature procedure for the synthesis of [{$Me_2NC(^iPrN)_2$}$_2Cu_2$], **2a**, (Scheme 1):[2g] This involved the dropwise addition of a stoichiometric amount of the appropriate carbodiimide to a solution of $LiNMe_2$ in tetrahydrofuran (THF) to form the lithiated guanidinates (**1a**−**d**) in situ. This solution was then added to a stoichiometric amount of CuCl, in the absence of light. After extraction into hexane and recrystallization at −28 °C, the desired Cu(I) guanidinate complex was isolated and fully characterized.

In the case of the isopropyl substituted guanidinate system **2a**, both ^{1}H and ^{13}C NMR data are consistent with that previously reported by Barry et al.[2g] As part of their study, a single crystal data set was collected at 120 K. For structural comparison with subsequent complexes described in this paper, the single crystal X-ray diffraction analysis of **2a** was also undertaken. As all structures in this study where measured at a temperature of 150 K we have included this data here as a direct comparison to subsequent structures within this study.

The ^{1}H NMR spectrum of the cyclohexyl substituted guanidinate complex, **2b**, in C_6D_6, shows the presence of four multiplet resonances associated with the four hydrogen environments in the {$C_6\underline{H}_{11}$} moiety between δ = 1.33−2.60 ppm and a sharp singlet at δ = 3.04 ppm for the {$N\underline{Me}_2$} protons. The ^{13}C NMR spectra also contains four resonances between δ = 25.2 and 54.5 ppm for the four unique carbon environments in the {$\underline{C}_6H_{11}$} moiety and resonances at δ = 58.7 and 161.7 ppm corresponding to the methyl amino carbon and the NCN central carbon, respectively.

Single crystal X-ray diffraction analysis reveals the molecular structure of **2b** to be a *di*-copper complex, which crystallizes with a full molecule in the asymmetric unit, in the triclinic $P\bar{1}$ space group, and is structurally similar to the isopropyl substituted guanidinate complex previously reported. Selected bond lengths, bond angles, and torsion angles for the *di*-copper complexes **2a** and **2b** are shown in Table 1, and the molecular structures of the two complexes are shown in Figure 1.

These complexes share many of the gross structural features of previously structurally characterized *di*-copper amidinate, guanidinate, and triazenide complexes.[2j] In each case, two metal centers are bridged by two guanidinate ligands in a μ,η^1,η^1-fashion with geometries about the two-coordinate metal centers that are approaching linearity [for **2a**: N(1)−Cu(1)−N(4) = 174.67 (9)°; for **2b**: N(1)−Cu(1)−N(4) = 170.59(11)° and N(2)−Cu(1)−N(5) = 170.58(11)°]. The deviation from linearity is presumably caused by variation in the internuclear separation of the Cu(I) centers (Figure 1, A-B). In both complexes, the metal−metal distances (see Table 1) which are comparable to related *di*-copper amindinate, guanidinate, and triazenide complexes,[2j] are significantly shorter than the sum of the

Scheme 1

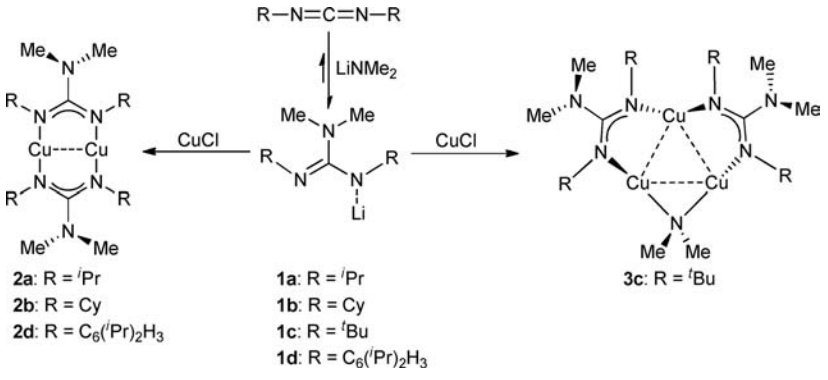

dx.doi.org/10.1021/ic201602m | Inorg. Chem. 2012, 51, 246−257

Table 1. Selected Geometric Data for Complexes 2a and 2b

2a		2b	
Selected Bond Lengths (Å)			
Cu(1)−N(1)	1.8745(19)	Cu(1)−N(1)	1.878(2)
Cu(1)−N(4)	1.8743(19)	Cu(1)−N(4)	1.881(3)
		Cu(2)−N(2)	1.872(2)
		Cu(2)−N(5)	1.876(2)
Cu(1)−Cu(1A)	2.4254(6)	Cu(1)−Cu(2)	2.4399(5)
N(1)−C(1)	1.335(3)	N(1)−C(1)	1.343(3)
N(1)−C(2)	1.484(3)	N(1)−C(2)	1.466(4)
		N(2)−C(1)	1.353(4)
		N(2)−C(8)	1.472(4)
N(3)−C(1)	1.406(3)	N(3)−C(1)	1.394(4)
N(4)−C(21)	1.344(3)	N(4)−C(21)	1.347(4)
N(4)−C(22)	1.476(3)	N(4)−C(22)	1.467(4)
		N(5)−C(21)	1.343(4)
		N(5)−C(28)	1.469(4)
N(6)−C(21)	1.384(5)	N(6)−C(21)	1.387(4)
Selected Bond Angles (deg)			
N(1)−Cu(1)−N(4)	174.67(9)	N(1)−Cu(1)−N(4)	170.59(11)
		N(2)−Cu(2)−N(5)	170.58(11)
N(1)−C(1)−N(1A)	120.3(3)	N(1)−C(1)−N(2)	120.2(3)
N(4)−C(21)−N(4A)	120.2(3)	N(4)−C(21)−N(5)	119.9(3)
Cu(1)−N(1)−C(2)	117.02(16)	Cu(1)−N(1)−C(2)	120.38(8)
		Cu(2)−N(2)−C(8)	120.84(19)
Cu(1)−N(4)−C(22)	120.07(8)	Cu(1)−N(4)−C(22)	120.3(2)
		Cu(2)−N(5)−C(28)	120.3(2)
Selected Torsion Angles (deg)			
N(1)−Cu(1)−Cu(1A)−N(1A)	18.2	N(1)−Cu(1)−Cu(2)−N(2)	29.0
N(4)−Cu(1)−Cu(1A)−N(4A)	15.4	N(4)−Cu(1)−Cu(2)−N(5)	29.7
N(1)−N(4)−N(4A)−N(1A)	16.5	N(1)−N(4)−N(5)−N(2)	27.0

van der Waals radii[16] of Cu (1.40 Å) suggesting the possible presence of d^{10}-d^{10} metallophilic bonding. While considerably weaker than related aurophilic interactions, closed shell cuprophilic interactions are now well established.[2j,17] While a full discussion of the nature of these interactions is beyond the scope of this paper,[18] these interaction are considered to play an important role in both solid state self-assembly and photoluminescence of polynuclear Cu(I) complexes.[17b,d,19] The Cu−N bond distances in both **2a** and **2b** are within the expected ranges for terminal Cu(I)−N bonds (see Table 1). Similarly the N−C bond lengths within the guanidinate ligands are also comparable to those observed in related systems.[5,7]

Unlike structurally related copper(I) amidinate complexes, which in the solid state have essentially planar *bi*cyclic cores,[2c,d] the central eight-membered $\{Cu_2N_4C_2\}$ ring formed by the two {NCN}-ligands and the $\{Cu_2\}$ unit in **2a** and **2b** deviate significantly from planarity. The root mean square (rms) deviation from the least-squares plane $\{Cu_2N_4C_2\}$ is 0.197(1) Å for **2a**, with the atoms N(1) and N(4) (also N(1)A and N(4)A) moving out of the plane by 0.286 Å and 0.270 Å, respectively. The rms deviation of the $\{Cu_2N_4C_2\}$ plane for **2b** is even larger (0.335(2) Å) with the atoms N(1), N(2), N(4), and N(5) moving out of the plane by 0.468, 0.474, 0.477, and 0.477 Å respectively. This deformation of the eight-membered ring can clearly be seen by viewing the complexes down the Cu−Cu axis (Figure 1C-D). Also noticeable in Figure 1 is the increased deformation of the $\{Cu_2N_4C_2\}$ plane in the cyclohexyl complex, **2b**, compared to the isopropyl analogue, **2a**, as highlighted by the torsion angles reported in table 1.

Similar, but significantly smaller twisting of guanidinate ligands has previously been attributed to delocalized π-bonding of the exocyclic $\{NR_2\}$ moiety in delocalized π-bonding with the $\{CN_2\}$ section of the guanidinate ligand. As noted earlier this should result in an imposed (and approximate) coplanarity of the $\{NR_2\}$ and $\{CN_2\}$ units in the ligand (Chart 1, structure B) as well as partial pyramidalization of the amide nitrogen atoms.[20] A close examination of the structural parameters for complexes **2a** and **2b** reveals that a change in the alkyl substituent (^{i}Pr to Cy) on the guanidinide ligand has little overall effect on the geometry about the $\{N-C(NMe_2)-N\}$ core of the ligand, with the C−N bond between the exocyclic $\{NR_2\}$ group and the $\{CN_2\}$ unit showing no evidence of increased multiple bond character [for **2a**: C(1)−N(3) 1.406(3) Å; C(21)−N(6) 1.384(5) Å, and for **2b**: C(1)−N(3) 1.394(4) Å; C(21)−N(6) 1.387(4) Å] or an increase in the pyramidal nature of the amide nitrogen atoms (see Table 2) as the alkyl substituents change.

Table 2. Additional Geometric Data for Complexes 2a and 2b

2a		2b	
Selected Torsion Angles (deg)			
N(1)−C(1)−N(3)−C(5)	43.9	N(1)−C(1)−N(3)−C(14)	43.0
N(1A)−C(1)−N(3)−C(5)	136.1	N(2)−C(1)−N(3)−C(14)	137.7
		N(1)−C(1)−N(3)−C(15)	35.7
		N(2)−C(1)−N(3)−C(15)	143.6
N(4)−C(21)−N(6)−C(25)	51.9	N(4)−C(21)−N(6)−C(34)	40.1
N(4)−C(21)−N(6)−C(25A)	128.1	N(5)−C(21)−N(6)−C(34)	140.2
		N(4)−C(21)−N(6)−C(35)	37.0
		N(5)−C(21)−N(6)−C(35)	142.6
Sum of Angles (about the Atom) (deg)			
N(1)	357.43	N(1)	358.56
		N(2)	356.52
N(4)	358.16	N(4)	356.78
		N(5)	357.51

We attribute the greater twisting of the $\{Cu_2N_4C_2\}$ plane in the cyclohexyl complex, **2b**, to the greater steric repulsion between adjacent amide nitrogen substituents.

Using an identical procedure to that used in the formation of **2a** and **2b**, the reaction of *N,N'*-di-*tert*-butyl-carbodiimide with $LiNMe_2$ was used to firm the in situ complex lithium guanidinate complex, $Li[(^tBuN)_2CNMe_2]$, **1c**. Reaction of this reaction mixture with CuCl in THF, followed by extraction into hexane and recrystallization resulted in the formation of colorless crystals. ^{1}H NMR spectroscopy of the product showed the presence of four singlet resonances at δ = 1.41, 1.48, 2.41, 3.09 ppm, in an 9:9:6:3 ratio, respectively, suggesting the presence of two different environments for the *tert*-butyl groups and two different $\{NMe_2\}$ environments which is consistent with the formation of a system of the general formula $[Cu_3\{Me_2NC(^tBuN)_2\}_2(NMe_2)]$, **3c**, rather than the desired *di*-copper system, $[(Me_2NC(^tBuN)_2)Cu]_2$.

Analysis of **3c** by single crystal X-ray diffraction confirms the complex to be a *tri*-copper cluster in which a central $\{Cu_3\}$ triangle is bridged by two $\{(^tBuN)_2CNMe_2\}$ ligands and by one $\{NMe_2\}$ unit, as shown in Figure 2. Selected bond lengths and angles are shown in Table 3. The complex **3c** crystallizes in the monoclinic space group $P2_1/n$, with a full molecule in the asymmetric unit cell. Successive attempts to synthesize the desired *di*-copper complex using the method outlined above resulted in the continual isolation of the *tri*-copper amide

dx.doi.org/10.1021/ic201602m | *Inorg. Chem.* 2012, 51, 246−257

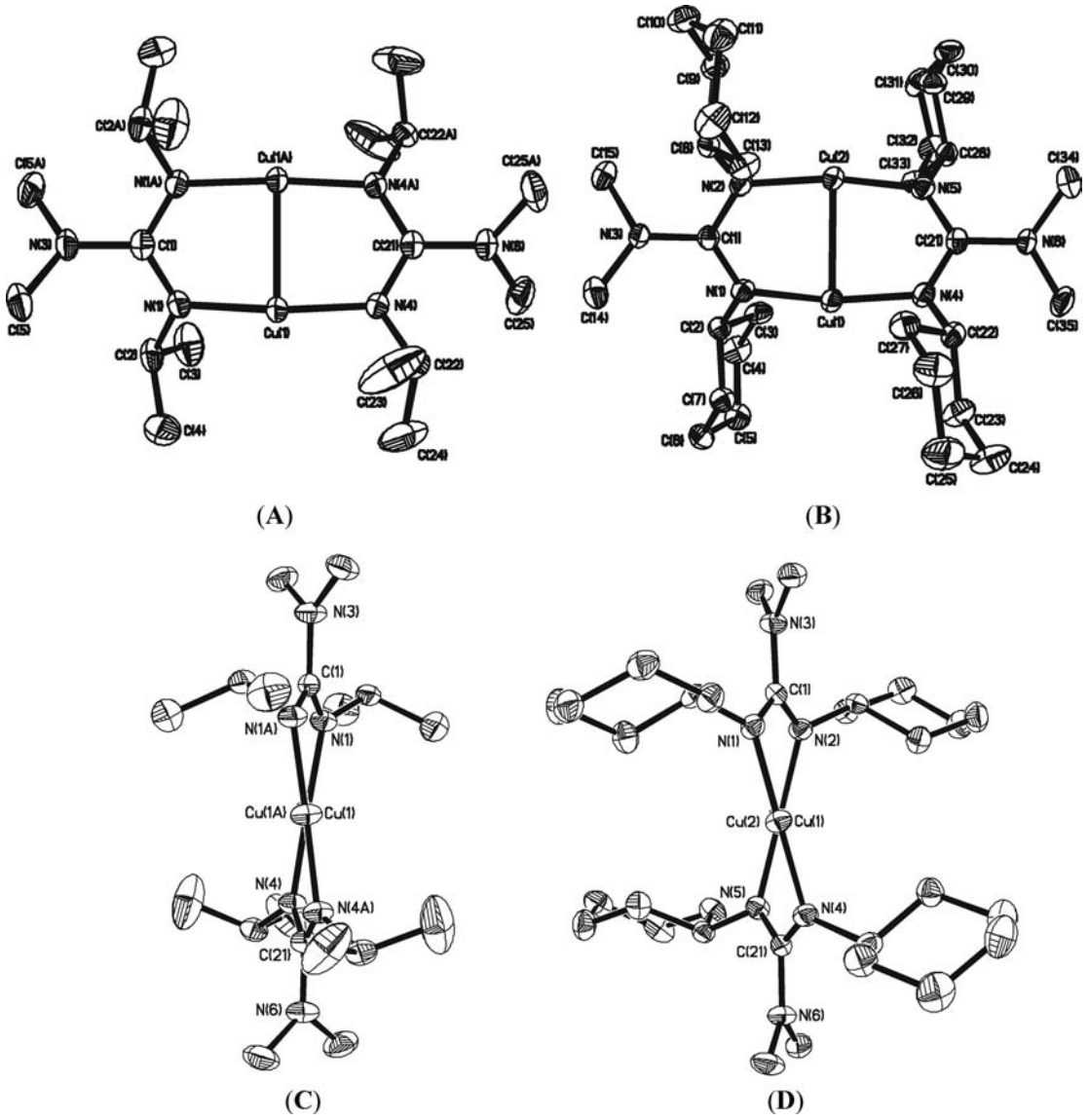

Figure 1. Diagram showing the molecular structures of the complexes **2a** (**A**) and **2b** (**B**): Figure 1A shows the molecular structure of one molecule of 2**a** (50% probability ellipsoids). Hydrogen atoms have been omitted for clarity. Symmetry transformations used to generate equivalent atoms: $-x, y, 1/2 - z$.; Figure 1B shows the molecular structure of **2b** (50% probability ellipsoids). Hydrogen atoms and solvent of crystallization have been omitted for clarity. Figures 1C and 1D show the molecular structures of the complexes viewed down the Cu−Cu axis emphasizing the deformation of planarity in the eight membered $\{Cu_2N_4C_2\}$ core.

complex, presumably a result of the continued presence of free $\{NMe_2\}$ in solution. In an attempt to eliminate the possibility of an error in the stoichiometry of the reaction, or the presence of free $Li[NMe_2]$, the lithium guanidinate salt, **1c**, was synthesized from the addition of a stoichiometric amount of *N,N′*-di-*tert*-butyl-carbodiimide to a suspension of lithium amide, $LiNMe_2$, in hexane and isolated by crystallization at −5 °C (Scheme 2).

As part of our study, the molecular structure of the lithium salt, **1c**, was determined by single crystal X-ray diffraction. The solid state structure of **1c** is shown in Figure 3 and selected bond lengths and angles in Table 4. In the solid state (and in the absence of donor solvent) **1c** exists as a tetrameric complex, $[Li_4\{(^tBuN)_2CNMe_2\}_4]$, crystallizing in monoclinic space group *C*2/*c* with half of the tetrameric unit in the asymmetric unit cell, the second half being generated by a 2-fold rotational axis. Within the tetramer there are two different lithium atom coordination environments: Li(1), which is coordinated to by two nitrogen atoms of different guanidinate ligands [Li(1)−N(2): 1.960(2) Å, Li(1)−N(5): 1.969(2) Å, N(2)−Li(1)−N(5): 157.83(12)°] and Li(2) which is similarly coordinated to two nitrogen atoms of different guanidinate ligands [Li(2)−N(1): 1.919(2) Å, Li(2)−N(4A): 1.907(2) Å, N(1)−Li(1)−N(4A): 170.80(15) °] but with slightly closer Li−N contacts. Each lithium atom is further supported by long agostic Li···H−C interactions[21] between the lithium centers and neighboring intramolecular methyl groups. Li(1) has four such interactions from about 2.19 to 2.28 Å, whereas Li(2) has four longer agostic interactions from about 2.45 to 2.72 Å, which is presumably a result of closer Li−N contacts.

The ^1H NMR spectrum of pure and isolated **1c**, in C_6D_6, shows the presence of several resonances, at δ = 1.14, 1.26, 1.36, and 1.41 ppm in the "*tert*-butyl" region and δ = 2.57, 2.65, and 2.82 ppm in the "NMe_2" region of the spectrum, suggesting the presence of more than one species in solution. Additionally, the relative intensities of these resonances appear to change with relative concentration of **1c** in solution, suggestive of possible equilibrium

dx.doi.org/10.1021/ic201602m | *Inorg. Chem.* 2012, 51, 246−257

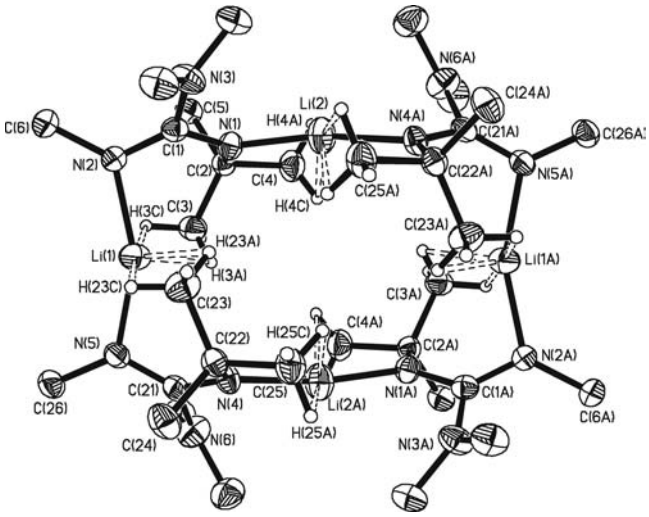

Figure 2. Diagram showing the molecular structures of the tetrameric lithium guanidinate complex **1c** (50% probability ellipsoids). Hydrogen atoms on methyl groups not involved in supporting Li···H−C interactions and methyl carbons attached to C(6), C(26), C(6A), and C(26A) have been omitted for clarity. Symmetry transformations used to generate equivalent atoms: $-x, y, 1/2 - z$.

Table 3. Selected Geometric Data for 1c

Selected Bond Lengths (Å) for **1c**			
Li(1)−N(2)	1.960(2)	Li(1)−C(3)	2.581(5)
Li(1)−N(5)	1.969(2)	Li(1)−H(3A)	2.270
Li(2)−N(1)	1.919(2)	Li(1)−H(3C)	2.192
Li(2)−N(4A)	1.907(2)	Li(1)−C(23)	2.580(5)
		Li(1)−H(23A)	2.278
C(1)−N(1)	1.3388(13)	Li(1)−H(23C)	2.152
C(1)−N(2)	1.4811(13	Li(2)−C(4)	2.747(5)
C(1)−N(3)		Li(2)−H(4A)	2.531
C(21)−N(4)	1.3417(13)	Li(2)−H(4C)	2.449
C(21)−N(5)	1.3275(13)	Li(2A)-C(25)	2.835(5)
C(21)−N(6)		Li(2A)−H(25A)	2.720
		Li(2A)−H(25C)	2.509
Selected Bond Angles (deg) for **1c**			
N(1)−C(1)−N(2)	120.59(8)	N(2)−Li(1)−N(5)	170.80(15)
N(4)−C(21)−N(5)	124.82(9)	N(1)−Li(2)−N(4A)	157.83(12)

Scheme 2

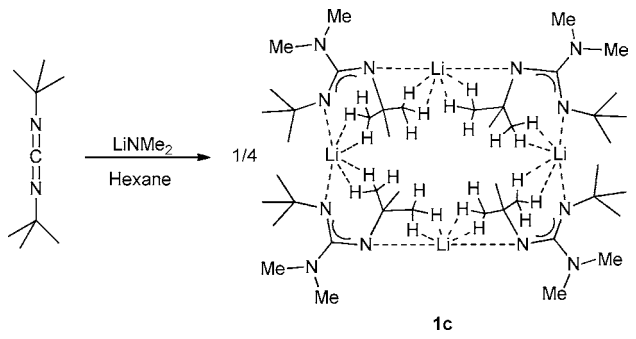

between **1c** and the starting materials (Scheme 3). Correspondingly, the ^{6}Li NMR spectrum shows the presence of two distinct broad resonances at 1.07 and 1.28 ppm respectively reinforcing this hypothesis. These observations are in direct contrast to di-isopropyl derivative **1a**, which displays only three resonances

Scheme 3

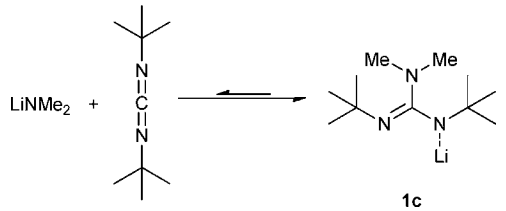

(as expected) in the ^{1}H NMR spectrum,[22] in both C_6D_6 and THF, suggesting any equilibrium between starting materials and products lies far toward the right-hand side of the equation.

In an attempt to elucidate any equilibrium processes present, variable temperature NMR studies of a sample of **1c** in d_8-THF were investigated. In contrast the room temperature ^{1}H NMR spectrum of **1c** in C_6D_6, the spectrum of **1c** in d_8-THF shows only four resonances: δ = 1.09 and 2.58 ppm which correspond to the {*t*-butyl} and {NMe_2} groups of **1c**, and resonances at δ = 1.23 and 2.75 ppm correspond to free *N,N′*-di-*tert*-butyl-carbodiimide and $LiNMe_2$ respectively. The ^{6}Li NMR spectra shows only one resonance at δ = 1.21 ppm indicative of a rapid exchange of lithium ions between **1c** and $LiNMe_2$. Between 320 and 270 K the ^{1}H spectra of **1c** in d_8-THF shows a significant change in the relative intensities of resonances: at 320 K the relative intensity ratios of **1c** to free *N,N′*-di-*tert*-butyl-carbodiimide is approximately 1:0.66. A reduction in temperature to 270 K results in an attendant change in the relative intensity ratio to 1:0.33. Below 270 K the ^{1}H NMR spectrum of **1c** in d_8-THF shows a splitting of the resonances associated with the complex **1c** into several new resonances, presumably because of a freezing out of *E* and *Z* isomerization processes. Kinetic studies of the exchange between *N,N′*-di-*tert*-butyl-carbodiimide and **1c** were studied using selective 1D-EXSY NMR spectroscopy following the method of Nikonov et al.[23] Spectra, run at 320, 326, 332, and 338 K respectively, were acquired at several mixing times, and a graph of signal intensity of the exchange peak, (normalized to the signal intensity of the irradiated peak) versus mixing time was found to be linear at short mixing times. Values for the rate constants (k) were taken from the slope of the graph. An Eyring plot of $\ln(k/T)$ versus $1/T$ provided an activation enthalpy of $\Delta H^{\ddagger}$ = 48.2 ± 18 kJ mol^{-1}, and an activation entropy of $\Delta S^{\ddagger}$ = 70.6 ± 6 J/K mol for the reaction (see Supporting Information for more detail).

Although the insertion of carbodiimides into lithium amide bonds has been widely studied and used extensively in synthesis,[1a] this study is to the best of our knowledge the first example of a reversible insertion of carbodiimides into a Li−N bond. Computational studies by Woo and Richardson have suggested that carbodiimide insertion into lithium amide complexes proceeds with relatively modest activation energies (less than 23 kcal mol^{-1}), with the ability of the migrating amide group to participate in delocalized π-bonding with the {NCN} backbone being a significant factor in the stability of intermediate species within the amide transfer.[24] In related work Chang and co-workers have shown experimentally *N,N′*-di-*tert*-butyl-carbodiimide insertion into Al−NR_2 bonds is unfavorable and reversible, an observation that has been rationalized in computational studies by Barry and co-workers on the basis of steric destabilization of intermediate transition states.[25]

Reaction of the isolated, and pure, lithium salt **1c** with a an excess of CuCl (1:6) in THF, followed by extraction into hexane and recrystallization at −28 °C yielded a crop of pale yellow crystals.

dx.doi.org/10.1021/ic201602m | *Inorg. Chem.* 2012, 51, 246−257

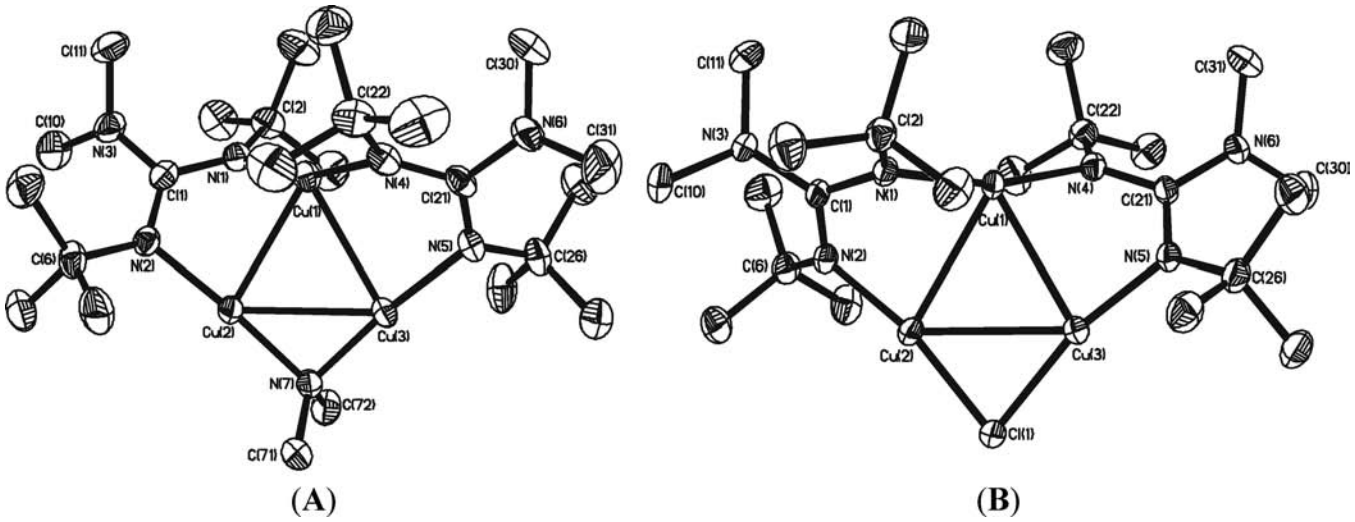

Figure 3. Diagram showing the molecular structures of the complexes **3c** (**A**) and **4c** (**B**) (50% probability ellipsoids). Hydrogen atoms have been omitted for clarity.

Table 4. Selected Geometric Data for 3c and 4c

3c		4c	
	Selected Bond Lengths (Å)		
Cu(1)–Cu(2)	2.7257(3)	Cu(1)–Cu(2)	2.7448(6)
Cu(2)–Cu(3)	2.7290(3)	Cu(2)–Cu(3)	2.7221(5)
Cu(1)–Cu(3)	2.6790(3)	Cu(1)–Cu(3)	2.6927(6)
Cu(1)–N(1)	1.8827(15)	Cu(1)–N(1)	1.8850(16)
Cu(1)–N(4)	1.8776(15)	Cu(1)–N(4)	1.8884(16)
Cu(2)–N(2)	1.8912(14)	Cu(2)–N(2)	1.8901(17)
Cu(3)–N(5)	1.8913(14)	Cu(3)–N(5)	1.8902(16)
Cu(2)–N(7)	1.8956(15)	Cu(2)–Cl(1)	2.1431(7)
Cu(3)–N(7)	1.8958(15)	Cu(3)–Cl(1)	2.1510(7)
C(1)–N(3)	1.392(2)	C(1)–N(3)	1.351(2)
C(21)–N(6)	1.391(2)	C(21)–N(6)	1.387(2)
	Selected Bond Angles (deg)		
Cu(1)–Cu(2)–Cu(3)	58.832(8)	Cu(1)–Cu(2)–Cu(3)	59.016(14)
Cu(2)–Cu(3)–Cu(1)	60.645(8)	Cu(2)–Cu(3)–Cu(1)	60.912(15)
Cu(3)–Cu(1)–Cu(2)	60.532(8)	Cu(3)–Cu(1)–Cu(2)	60.072(8)
Cu(2)–N(7)–Cu(3)	92.07(6)	Cu(2)–Cl(1)–Cu(3)	78.680(19)
N(1)–Cu(1)–N(4)	160.55(7)	N(1)–Cu(1)–N(4)	164.36(7)
N(2)–Cu(1)–N(7)	175.79(7)	N(2)–Cu(1)–Cl(1)	168.82(5)
N(5)–Cu(1)–N(7)	171.59(6)	N(5)–Cu(1)–Cl(1)	166.73(5)
N(1)–C(1)–N(2)	117.64(16)	N(1)–C(1)–N(2)	117.71(17)
N(4)–C(21)–N(5)	118.54(15)	N(4)–C(21)–N(5)	117.95(16)
	Selected Torsion Angles (deg)		
N(1)–Cu(1)–Cu(2)–N(2)	42.63(7)	N(1)–Cu(1)–Cu(2)–N(2)	42.47(7)
N(4)–Cu(1)–Cu(3)–N(5)	36.61(7)	N(4)–Cu(1)–Cu(3)–N(5)	37.96(8)

The ^{1}H NMR spectrum of the product revealed the presence of three sharp singlet resonances at δ = 1.35, 1.40, and 2.38 ppm, respectively in a 9:9:6 intensity ratio indicating two different magnetic environments for the *tert*-butyl groups. The absence of an additional resonance corresponding to addition $\{NMe_2\}$ was consistent with the possible formation of the desired $[Cu_2(\mathbf{L}^3)_2]$ complex.

However, determination of the product's molecular structure revealed the complex to be a new *tri*-copper complex, with a comparable central $\{Cu_3\}$-triangle bridged by two $\{(^tBuN)_2CNMe_2\}$ ligands and one chlorine atom to form $[Cu_3\{Me_2NC(^tBuN)_2\}_2(\mu\text{-Cl})]$ (**4c**) (Scheme 4) which crystallizes in the triclinic space group $P\bar{1}$ and contains a full molecule in the asymmetric unit cell. The molecular structure of **4c** is also shown Figure 3, and selected bond lengths and angles are shown in Table 4.

Scheme 4

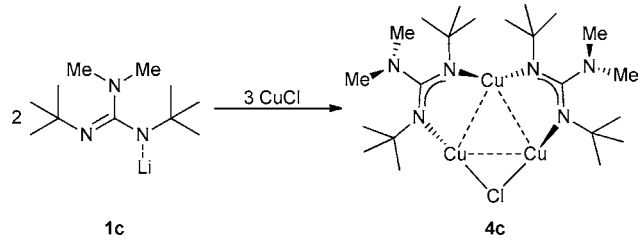

The triangular $\{Cu_3\}$ cores (Figure 4) of both *tri*-copper complexes, **3c** and **4c**, have approximately isoscelean geometry (see Table 4 for Cu–Cu bond lengths). Surprisingly in both cases the shortest Cu–Cu distance is bridged by a guanidinate ligand rather than a $\{NMe_2\}$ or {Cl} moiety, as is the case in the structurally related trimethylsilyl-substituted guanidinate derivative $[Cu_3\{Me_2NC(Me_3SiN)_2\}_2(\mu\text{-}NMe_2)]$.[26]

In both complexes the Cu–Cu edges are significantly longer than that observed in either **2a** or **2b**. As with **2a** and **2b**, the Cu–N distances are in the range expected for comparable copper-amidinate and -triazenide complexes,[2j] (see Table 4)

The bridging guanidinate ligands of both complexes form two twisted five-membered $\{Cu_2N_2C\}$ rings. As an example, Figure 3 shows the skeleton framework of the complex **3c** viewed down the Cu(2)–Cu(3) and N(7)–Cu(1) vectors, illustrating the twisting that is experienced by the $\{L^3\}$ ligand in both **3c** and **4c**. A comparison of the torsion angles observed in $[Cu_3(\mathbf{L}^3)_2(\mu\text{-}NMe_2)]$; N(1)–Cu(1)–Cu(2)–N(2) (42.63(7)°), N(4)–Cu(1)–Cu(3)–N(5) (36.61(7)°) and $[Cu_3(\mathbf{L}^3)_2(\mu\text{-Cl})]$; N(1)–Cu(1)–Cu(2)–N(2) (42.47(7)°), N(4)–Cu(1)–Cu(3)–N(5) (37.96(7)°), indicate significantly more distortion within the *tri*-copper complexes than in the dicopper systems (cf. 18.2° and 15.4° for **2a**, 29.0° and 29.7° for **2b**]). It is also notable that the smaller torsion angles are associated with the short Cu(1)–Cu(3) edge in both

dx.doi.org/10.1021/ic201602m | *Inorg. Chem.* 2012, 51, 246–257

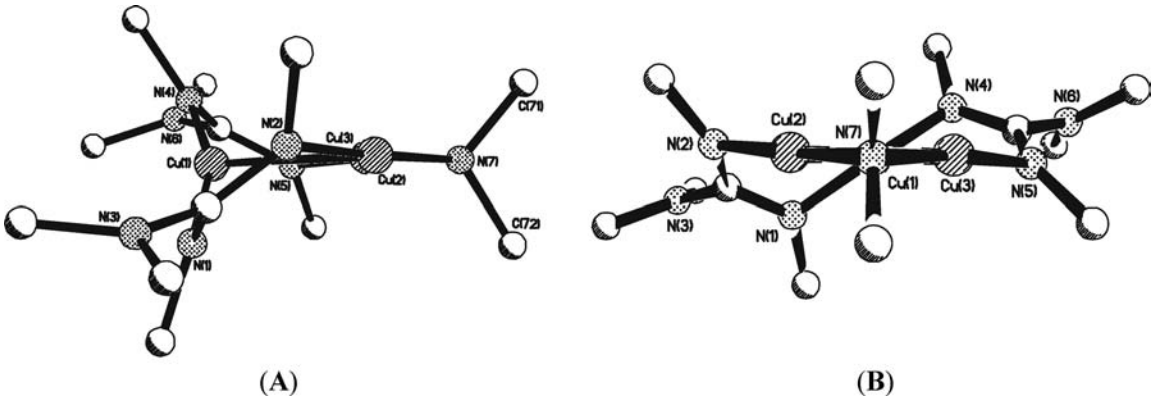

Figure 4. Diagram showing the core of **3c**: a view along the approximate Cu(2)−Cu(3) vector (**A**), and down the N(7)−Cu(1) vector (**B**) pictographically illustrating twisting of the guanidinate ligands. Selected angles: N(1)−Cu(1)−Cu(2)−N(3): 42.63(7)°, N(4)−Cu(1)−Cu(3)−N(6): 36.61(7)°.

clusters. The increased twisting observed in the *tert*-butyl derivatives is again attributed to the increased steric repulsion experienced within the ligand sphere of the complexes compared to the cyclohexyl and iso-propyl derivatives respectively.

In both **3c** and **4c** one unique edge of the $\{Cu_3\}$ cluster is bridged by either a $\{NMe_2\}$ moiety [Cu(2)−N(7); 1.9856(15) Å, Cu(3)−N(7); 1.8958(15) Å] or {Cl} atom [Cu(2)−Cl(1); 2.1431(7) Å, Cu(3)−Cl(1); 2.1510(7) Å] with bond lengths that are comparable to related Cu(I) systems with edge bridging amide groups[27] or chlorine atoms.[28] The longer bond lengths between the Cu(2)−Cu(3) edge and the bridging units ($\{NMe_2\}$ or {Cl}) are also reflected in the Cu(2)−E−Cu(3) angle [E = N(7); 92.07(6), E = Cl(1); 78.680(19)].

In the case of **3c** the $\{NMe_2\}$ moiety is orientated approximately perpendicular [89.25(15)°] to the plane of the *tri*-copper unit, reflecting the three-center two-electron (3c-2e) bonding between Cu(1), Cu(3) and the $\{NMe_2\}$ unit. This is a common feature in *tri*- and *tetra*-copper based clusters containing edge bridging amide groups,[27,29] The range for Cu−Cu distances bridged by 3c-2e bonds has previously been shown to be 2.702(2)−2.742(2) Å in planar $[Cu_4(NR_2)_4]$ systems[27] which are comparable to the Cu(1)−Cu(3) bridged edges in both **3c** and **4c**.

Successive attempts to produce the *di*-copper complex $[Cu_2\{Me_2NC(^tBuN)_2\}_2]$ by reacting **1c** with varying excess amounts (2:1 and 3:2) of CuCl in different solvents (diethylether or tetrahydrofuran), resulted in further isolation of the *tri*-copper system **4c**.

It is our belief that the steric demands caused by the bulky *tert*-butyl substituents is such that the putative dimeric complex $[\{Me_2NC(^tBuN)_2\}_2Cu_2]$ is unstable, leading to an opening of the metallo-ligand framework and the incorporation of an additional $\{CuNMe_2\}$ or {CuCl} unit to form the a *tri*-copper systems with reduced steric strain and twist. It is not clear why these products should be formed over a possible *tri*-copper complex $[Cu_3[\{Me_2NC(^tBuN)_2\}_3]$ as is the case in related silver amidinate, guanidinate, and triazenide systems.[2a,j,k] Variable temperature ^{1}H NMR studies of both *tri*-copper complexes reported here show no evidence of equilibrium between dimeric and trimeric species or evidence of ligand scrambling at elevated temperatures.

In this context, it is interesting to note that while cyclohexyl and iso-propyl copper(I) amidinates complex have been studied by Gordon and co-workers as CVD and ALD precursors,[2d,e] the related *tert*-butyl substituted copper(I) amidinate analogues, that is, $\{(^tBu\text{-}N)_2CR\}$ (R = Me or ^{t}Bu), have never been reported despite the commercial availability of *N,N′*-di-*tert*-butyl-carbodiimide.

Initial attempts to synthesize the 2,6-*di*isopropylphenyl substituted guanidinate derivative **2d** focused on the in situ formation of the lithium guanidinate salt **1d** in reactions that are analogous to those used in the synthesis of **2a** and **2b**. However, this reaction resulted in the formation of a highly air and oxygen-sensitive reaction mixture which would rapidly react with trace amounts of oxygen to form an intensely green colored solution. In an attempt to reduce the overall reaction time with Cu(I) salts to a minimum, the lithium precursor **1d** was synthesized and isolated prior to reaction with copper chloride.

Addition of a stoichiometric amount of *N,N′*-bis-2,6-*di*-isopropylphenyl-carbodiimide to a suspension of lithium amide, $LiNMe_2$, in hexane, resulted in immediate reaction and formation of a colorless solution. Filtration of the reaction mixture, to remove insoluble material, followed by cooling to −5 °C resulted in the formation of a crop of colorless crystals (Scheme 5).

Scheme 5

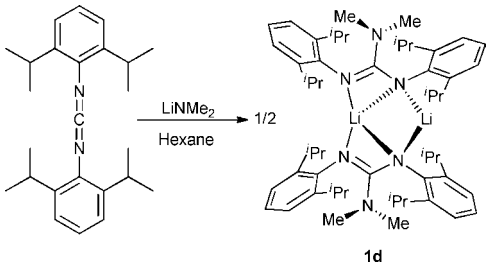

Analysis of the lithium salt by single crystal X-ray diffraction reveals the system to be a dimeric complex that can be represented formulaically as $[Li_2\{Me_2NC(DipN)_2\}_2]$ (Dip = 2,6-*di*isopropylphenyl), and which crystallizes in the monoclinic space group $P2_1/n$, containing two independent whole molecules of the *di*-lithium salt in the asymmetric unit cell. The two dimer molecules differ only in the relative orientations of the 2,6-*di*isopropylphenyl substituents and are equivalent, within experimental error, to each other. Figure 5 shows the molecular structure of one of the two dimer molecules of **1d** in the asymmetric unit cell, and is taken as representative of both molecules that are present. Selected bond lengths and angles for **1d** are reported in Table 5.

dx.doi.org/10.1021/ic201602m | *Inorg. Chem.* 2012, 51, 246−257

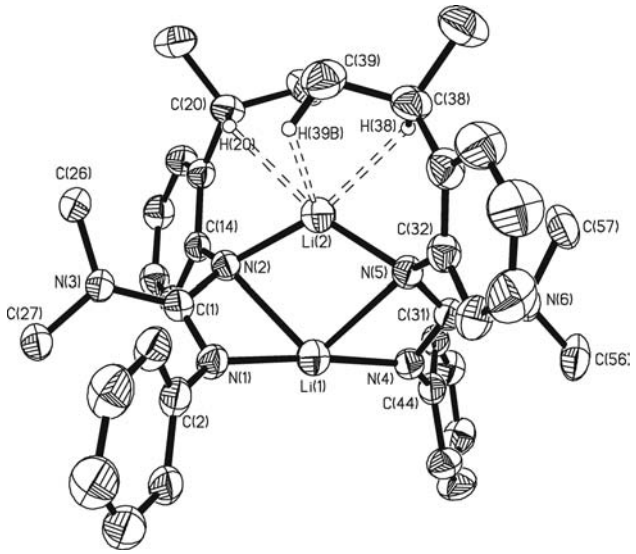

Figure 5. Diagram showing the molecular structures of the dimeric lithium guanidinate complex **1d** (50% probability ellipsoids). Hydrogen atoms not involved in supporting Li···H−C interactions and isopropyl groups {$CHMe_2$} attached to C(3), C(7), C(19), C(37), C(45), and C(49) have been omitted for clarity.

Table 5. Selected Geometric Data for 1d

Selected Bond Lengths (Å) for **1d**			
Li(1)−N(1)	1.977(3)	N(1)−C(1)	1.324(2)
Li(1)−N(2)	2.293(3)	N(2)−C(1)	1.424(2)
Li(1)−N(4)	1.979(3)	N(3)−C(1)	1.381(2)
Li(1)−N(5)	2.253(3)	N(4)−C(31)	1.325(2)
Li(2)−N(2)	1.928(4)	N(5)−C(31)	1.368(2)
Li(2)−N(5)	1.923(4)	N(6)−C(31)	1.375(2)
Li(1)···Li(2)	2.452(5)		
Li(2)−C(20)	2.882(7)	Li(2)−C(39)	2.865(7)
Li(2)−H(20)	2.257	Li(2)−C(39B)	2.298
Li(2)−C(38)	2.809(7)		
Li(2)−H(38)	2.194		
Selected Bond Angles (deg) for **1d**			
N(1)−Li(1)−N(4)	174.82(19)	N(1)−Li(1)−N(2)	64.43(10)
N(2)−Li(1)−N(5)	95.77(13)	N(4)−Li(2)−N(5)	64.96(10)
N(2)−Li(2)−N(5)	122.31(18)	Li(1)−N(2)−Li(2)	70.42(13)
		Li(1)−N(5)−Li(2)	71.42(13)
N(1)−C(1)−N(2)	116.66(14)		
N(4)−C(31)−N(5)	116.02(14)		

Within the molecular dimer there are two different lithium coordination environments. Li(1) is coordinated by two chelating guanidinate ligands. While the ligand based around C(1) possesses much more clearly localized bonding, the ligand based around C(31) is more delocalized, as can be seen from the relative C−N bond lengths (Table 5).

The relative orientation of the system is such that there are two short Li−N contacts [Li(1)−N(1): 1.977(3) Å and Li(1)−N(4): 1.967(3) Å] in an environment that is approaching linearity [N(1)−Li(1)−N(4): 174.82(19)°] and two longer Li−N contacts [Li(1)−N(2): 2.293(3) Å and Li(1)−N(5): 2.253(3) Å] with a more bent geometry [N(2)−Li(1)−N(5): 95.77(13)°]. The second lithium atom, Li(2), is coordinated by the two more distant nitrogen atoms, N(2) and N(5), in a somewhat bent coordination environment [Li(2)−N(2): 1.928(4) Å and Li(2)−N(5): 1.923(4) Å; N(2)−Li(2)−N(5): 122.31(18)°]. Although both lithium environments are different, the Li−N contacts lie within the range expected for lithium amidinate and guanidinate systems.[21b,30] The coordination sphere of the more exposed Li(2) metals center is completed by three agostic interactions (see Figure 5) [between 2.194 and 2.298 Å] to ligand hydrogen atoms.

Reaction of the **1d** with stoichiometric amounts of CuCl in THF, and in the absence of light, yielded a pale yellow solution which was highly susceptible to oxidation by trace amounts of oxygen. Removal of the solvent under reduced pressure followed by extraction into hot hexane, and filtration yielded a pale yellow solution which on standing at −28 °C produced yellow crystals. ^{1}H NMR spectroscopy of the product showed the presence of four doublet resonances at δ = 0.71, 1.19, 1.29, and 1.95 ppm, one singlet resonance at 1.99 ppm, two septet resonances at 3.53 and 3.81 ppm, and a range of multiplets between 6.96 and 7.14 ppm in the relative intensity ratio of 3:3:3:3:3:1:1:3, suggesting a coordination environment for the guanidinate ligand system in which each methyl and methine group attached to a 2,6-*di*isopropyl phenyl substituent is in a different magnetic environment, consistent with the formation of the *di*-copper complex **2d**. A similar resonance pattern has been observed for the related 2,6-*di*isopropyl phenyl substituted copper triazenide complex.[2j]

Crystals of **2d** suitable for single crystal X-ray diffraction have been grown from two different solvents, hexane and toluene. In both cases poor quality crystals have produced low quality data. This, combined with inherent disorder with the isopropyl groups on the ligand, has meant that to-date it has not proved possible to find a structural model that allows us to place any confidence on the bond lengths and angles for the complex. However, after collecting and partially solving four data sets, we are confident that the geometry of the heavy atoms is that shown in Figure 6.

While little confidence can be placed on the accuracy of bond lengths and angles in **2d**, it is clear that the complex is structurally comparable to both **2a** and **2b**, adopting a dimeric structure in the solid state. Unlike **2a** and **2b**, there is no clear evidence of twisting of the guanidinate ligand, as can be seen from Figure 7 which shows views down the N(3)−C(1)−C(31)−N(6) vector and the Cu(1)−Cu(2) vector respectively. It can also be clearly seen from Figure 7 that relief from the steric repulsion induced by the close proximity of the 2,6-diisopropylphenyl groups occurs as a result of pyramidalization of the nitrogen atom to which these groups are attached.

Thermolysis. The copper guanidinate compounds **2a**, **2b**, **2d**, **3c**, and **4c** were studied to determine their thermal chemistry.

Thermogravimetric analysis (TGA) data, under argon, were collected for each compound to determine their volatility and appraise their decomposition profiles. While all five compounds showed decomposition profiles with residues less than 25%, and indicated on the basis of mass loss the formation of copper metal, the decomposition TGA profiles of the *tri*-copper complexes **3c** and **4c**, and the aromatic containing complex **2d**, suggest the compounds decompose in a series of multistep processes over a temperature range of 150−350 °C.

The TGAs of **2a** and **2b** are shown in Chart 3. Barry et al. have previously reported the onset of volatility for **2a** as 105 °C,

dx.doi.org/10.1021/ic201602m | *Inorg. Chem.* 2012, 51, 246−257

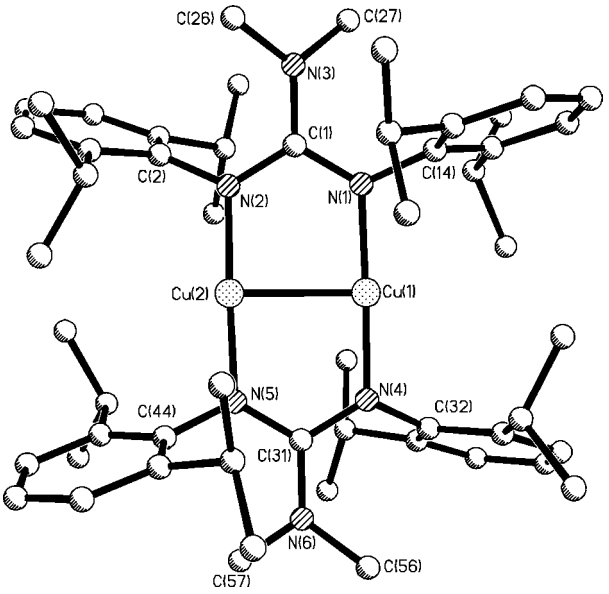

Figure 6. Molecular structure of **2d**, showing the gross structural features of the complex within the disordered structure. Only the heavy atoms are shown, drawn as arbitrary sized spheres.

a value that is consistent with our results.[2g] However, in our hands TGA mass residue levels for **2a** are approximately 25%, which is slightly lower than the value that corresponds to the decomposition of the species to provide pure copper (27%), and significantly higher than the residue levels of 1.8% reported by Barry et al.

In contrast, **2b** shows a considerably higher onset of mass loss at approximately 176 °C. After the onset of volatilization, both systems show relatively sharp and clean decomposition profiles to give stable residues. For **2b** the stable residue reached is higher than a value that would correspond to pure copper, 26% (cf. 20%), indicating some contamination in the decomposition product.

Chart 3. Thermogravimetric Analyses of 2a (Light Line) and 2b (Dark Line)

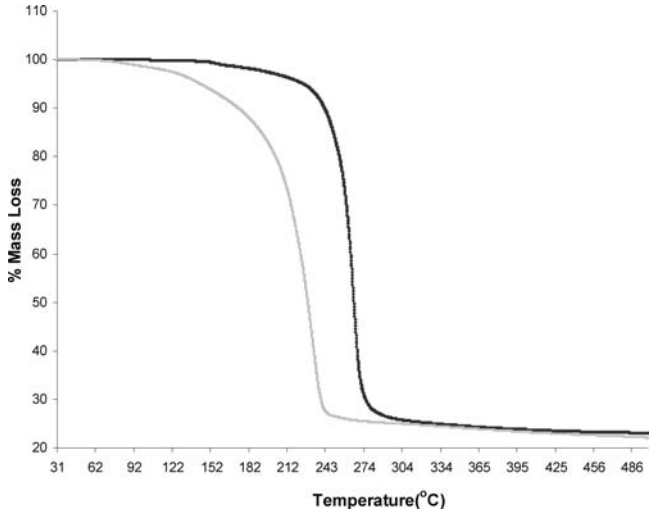

CONCLUSIONS

Reported herein are the structures of several novel Cu(I) complexes containing metal−metal interactions supported by progressively more sterically demanding guanidinate ligands.

Reactions of CuCl with lithium guanidinate complexes Li[{Me_2-NC(^{i}PrN)$_2$}], Li[[{Me_2NC(CyN)$_2$}], and Li[[{Me_2NC-(DipN)$_2$}] provide the homoleptic complexes **2a**, **2b**, and **2d**, respectively, which have been structurally characterized. For the complexes **2a** and **2b**, increasing the relative size of the guanidinate substituent has a significant effect on the molecular structure of the resultant dimers, specifically with respect to the twisting of the guanidinate substituents and loss of planarity across the dimer. In the case of **2d**, steric relief is achieved by pyramidalization of the aryl substituted nitrogen atoms of the guanidinate ligand, a feature which has previously been observed in the related triazenide system.[2j]

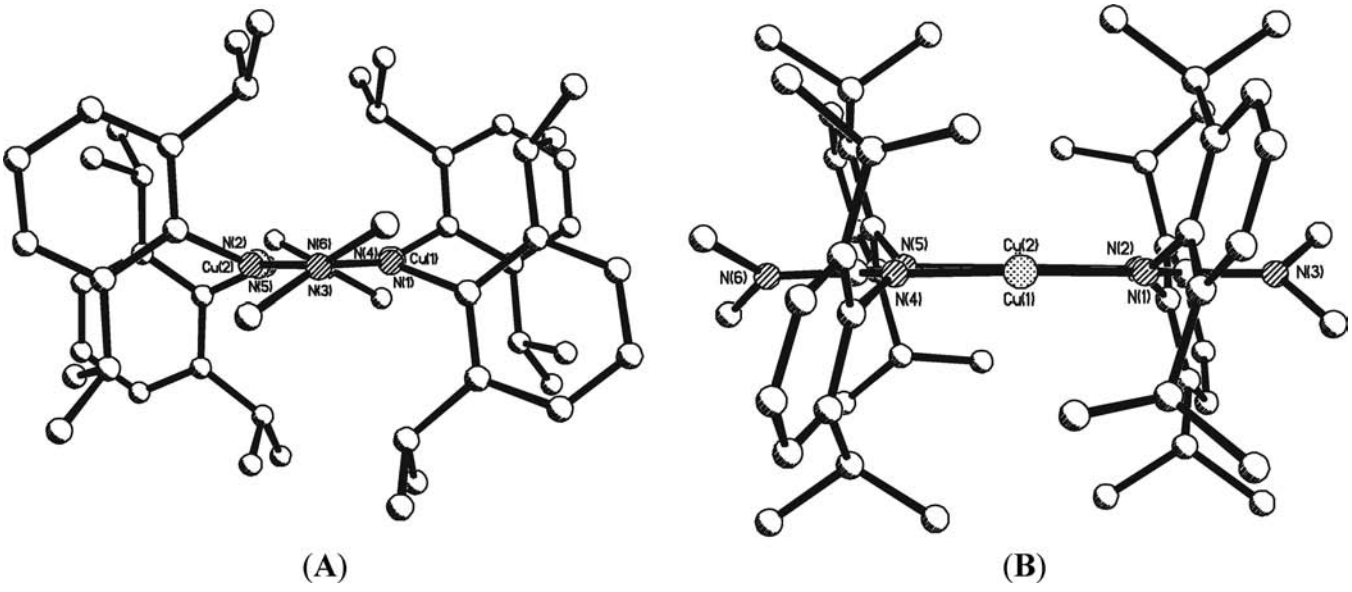

Figure 7. Views of the complex **2d** down the N(3)−N(6) (**A**) and Cu(1)−Cu(2) (**B**) vectors respectively, highlighting the relative planarity of the central {$Cu_2N_4C_2$} core and the lack of twisting of the guanidinate about the Cu−Cu bond.

dx.doi.org/10.1021/ic201602m | *Inorg. Chem.* 2012, 51, 246−257

In contrast, the reaction of the *tert*-butyl substituted guanidinate system **1c** (formed in situ) with CuCl results in the serendipitous formation of a novel Cu(I) *tri*-metallic system, **3c**.

Closer inspection of the solution state properties of **1c** reveal a previously unreported equilibrium between the lithium guanidinate complex **1c** and free *N,N′*-di-*tert*-butyl-carbodiimide and $LiNMe_2$, for which activation enthalpy and activation entropy values have been calculated using 1D-EXSY NMR spectroscopy. The observation that **1c** participates in this equilibrium process explains why $\{NMe_2\}$ is available in solution for incorporation into the complex **3c**.

The precise reasons for this difference in reactivity between the guanidinate systems **1a**−**1d** (**1a**, **1b**, and **1d** show no evidence of equilibrium processes) are not fully understood, but it is possible to speculate that there is a fine balance between steric and electronic considerations. Complexes containing the *tert*-butyl guanidinate unit $\{Me_2NC(^tBuN)_2\}$, are expected to be highly sterically hindered, which goes some way to explaining the observed equilibria of the lithium complex **1c**. This steric hindrance is relieved somewhat by twisting of the guanidinate ligand as observed in the *tri*-copper systems **3c** and **4c**.

Despite the fact that our initial intent was to synthesis the dimeric system $[Cu_2\{Me_2NC(^tBuN)_2\}_2]$, we now believe that the steric repulsion between adjacent *tert*-butyl groups across the central $\{Cu_2\}$ unit is too great for this system to be stable. Twisting of the guanidinate backbone, along with scavenging of free "$CuNMe_2$" or "CuCl" allows the steric strain to be relieved resulting in the formation and isolation of the *tri*-metallic systems $[Cu_3\{Me_2NC(^tBuN)_2\}_2(\mu\text{-}NMe_2)]$ (**3c**) and $[Cu_3\{Me_2NC(^tBuN)_2\}_2(\mu\text{-}Cl)]$ (**4c**).

While all five Cu(I) complexes described here have been analyzed by thermogravimetric analysis, only **2a** and **2b** show potential as CVD or ALD precursors because of their clean decomposition pathways and relative onsets of volatilization.

EXPERIMENTAL SECTION

General Procedures. Elemental analyses were performed by Elemental Microanalysis Ltd., Okehampton, Devon, U.K. ^1H and ^{13}C NMR spectra were recorded on a Bruker Avance 300 MHz FT−NMR spectrometer, as saturated solutions in d_2-CD_2Cl_2; chemical shifts are quoted in units of parts per million (ppm), relative to Me_4Si (^1H, ^{13}C); coupling constants are in hertz (Hz).

All reactions were carried out under an inert atmosphere, and in the absence of light, using standard Schlenk techniques. Solvents were dried over activated alumina columns using an Innovative Technology solvent purification system (SPS) and degassed under an argon atmosphere. All other reagents were purchased from commercial sources.

Thermogravimetric analysis (TGA) of the complexes was performed at SAFC Hitech, Bromborough, U.K., using a Shimadzu TGA-51 Thermogravimetric Analyzer. Data points were collected every second at a ramp rate of 20 °C min^{-1} in a flowing (50 mL min^{-1}) N_2 stream.

*Synthesis of (**1c**).* In a dry Schlenk, hexane (20 mL) was added to lithium dimethylamide (0.10 g, 2.0 mmol) to give a cream/pale yellow suspension. To this, *N,N′*-di-*tert*-butyl-carbodiimide (0.39 mL, 2.0 mmol) was added dropwise, and the reaction mixture left to stir for 2 h. The resulting clear solution was heated to reflux and filtered, via cannula, into a clean Schlenk. Storage of the reaction mixture at −5 °C resulted in the formation of a crop of colorless crystals which were isolated by filtration. (0.36 g, 87%). ^1H NMR (d_8-THF, 300.22 MHz) δ: 1.09 (s, 9H, $C(CH_3)_3$ of **1c**), 1.23 (s, 9H, $C(CH_3)_3$ of free ^{t}Bu-N=C=N-^{t}Bu), 2.58 (s, 6H, $N(CH_3)_2$ of **1c**), 2.75 (s, 6H, $N(CH_3)_2$ of free $LiNMe_2$); ^{13}C NMR (d_8-THF, 75.49 MHz) δ: 31.4 ($C(CH_3)_3$ of free ^{t}Bu-N=C=N-^{t}Bu), 33.5 ($C(CH_3)_3$ of **1c**), 42.3 ($C(CH_3)_3$ of **1c**), 47.9 ($C(CH_3)_3$ of free ^{t}Bu-N=C=N-^{t}Bu) 51.5 ($N(CH_3)_2$ of **1c**), 54.7 ($N(CH_3)_2$ of free $LiNMe_2$), 139.2 (NCN of free ^{t}Bu-N=C=N-^{t}Bu), 167.6 (NCN of **1c**); ^6Li NMR (C_6D_6, 155.5 MHz) δ: 1.21 (s, 1Li).

*Synthesis of (**1d**).* Complex **1d** was synthesized in an analogous fashion to **1c** using *N,N′*-bis-2,6-*di*isopropylphenyl-carbodiimide (0.72 g, 2.0 mmol). Yield = 0.81 g, 98%. ^1H NMR (C_6D_6, 300.22 MHz) δ: 1.04 (d, 12H, J = 7 Hz, $(CH_3)CH(CH_3)$), 1.22 (d, 12H, J = 7 Hz, $(CH_3)CH(CH_3)$), 2.23 (s, 6H, $N(CH_3)_2$), 3.43 (m, 4H, (CH_3)-$CH(CH_3)$), 6.98−7.06 (m, 6H, CH_{Ar}); ^{13}C NMR (C_6D_6, 75.49 MHz) δ: 23.4 ($CH(CH_3)_2$), 25.6 ($CH(CH_3)_2$), 28.5 ($CH(CH_3)_2$), 40.2 ($N(CH_3)_2$), 122.5 (CH), 124.2 (CH), 124.2 (CH), 141.5 (C-CH-$(Me)_2$), 146.8 (C-CH-$(Me)_2$), 144.3 (N-C), 167.5 (NCN). ^6Li NMR (C_6D_6, 155.5 MHz) δ: 2.83 (s, 1Li).

*Synthesis of (**2b**).* In a dry Schlenk, tetrahydrofuran (40 mL) was added to lithium dimethylamide (0.77 g, 15.0 mmol) to give a pale yellow slurry. *N,N′*-dicyclohexyl-carbodiimide (3.09 g, 15.0 mmol) was then added dropwise via syringe, and the reaction mixture left to stir for 2 h. The resulting pale yellow solution was transferred by cannula to a Schlenk containing copper(I) chloride (1.49 g, 15.0 mmol), and the reaction mixture allowed to stir for 18 h, after which time the volatiles were removed under reduced pressure. Hexane (20 mL) was added to the resultant residue and left to stir for 15 min, and was subsequently removed under reduced pressure. This process was repeated twice to remove any residual tetrahydrofuran. The product was then extracted into hexane and filtered through Celite, and the resultant filtrate was concentrated. Storage of the solution at −28 °C facilitated the growth of colorless crystals suitable for single crystal X-ray diffraction (2.90 g, 62%). Mp 152 °C. Elemental analysis: calcd. for $C_{30}H_{58}Cu_2N_6$ (%):C, 57.39, H: 8.99, N, 13.38, found: C, 56.92, H, 8.91, N, 13.01%. ^1H NMR (C_6D_6, 300.22 MHz) δ: 1.33 (m, 8H, CH_2), 1.68 (m, 16H, $(CH_2)_2$), 2.06 (m, 16H, $(CH_2)_2$), 2.60 (s, 12H, $N(CH_3)_2$), 3.04 (m, 4H, NCH); ^{13}C NMR ($CDCl_3$, 75.49 MHz) δ: 25.2 (CH_2), 25.6 ($(CH_2)_2$), 40.0 ($(CH_2)_2$), 54.5 (NCH), 58.7 ($N(CH_3)_2$), 161.7 (NCN).

*Synthesis of (**2d**).* To a dry Schlenk, tetrahydrofuran (40 mL) was added to a mixture of lithium dimethylamide (0.77 g, 15.0 mmol) and *N,N′*-bis-2,6-*di*isopropylphenyl-carbodiimide (5.44 g, 15.0 mmol) to give a pale yellow solution. The reaction mixture was left to stir for 2 h after which the solution was transferred by cannula to a Schlenk containing copper(I) chloride (1.49 g, 15.0 mmol). The reaction mixture was allowed to stir for 18 h, after which time the volatiles were removed under reduced pressure. Hexane (20 mL) was added to the resultant residue and left to stir for 15 min, after which time the hexane was removed under reduced pressure. The process was repeated twice to remove any residual tetrahydrofuran. The product was then extracted into hexane and filtered through Celite. The resultant filtrate was concentrated, and storage of the material at −28 °C facilitated the growth of yellow crystals suitable for single crystal X-ray diffraction (5.10 g, 72.4%). Mp 111 °C (dec). Elemental analysis: calcd. for $C_{54}H_{80}Cu_2N_6$ (%): C, 68.97, H: 8.58, N, 8.94, found: C, 69.08, H, 8.34, N, 8.84%. ^1H NMR (C_6D_6, 300.22 MHz) δ: 0.71 (d, 12H, J = 7 Hz, $(CH(CH_3)_2)$, 1.19 (d, 12H, J = 7 Hz, $CH(CH_3)_2$), 1.28 (d, 12H, J = 7 Hz, $CH(CH_3)_2$),1.59 (d, 12H, J = 7 Hz, $CH(CH_3)_2$), 1.99 (s, 12H, $N(CH_3)_2$), 3.53 (sept, 4H, J = 7 Hz, $CH(CH_3)_2$), 3.81 (sept, 4H, J = 7 Hz, $CH(CH_3)_2$), 6.96−7.14 (m, 12H, CH_{Ar}); ^{13}C NMR ($CDCl_3$, 75.49 MHz) δ: 22.9 ($CH(CH_3)_2$), 23.1, ($CH(CH_3)_2$), 24.2 (CH-$(CH_3)_2$), 25.7 ($CH(CH_3)_2$), 27.9 ($CH(CH_3)_2$), 28.1 ($CH(CH_3)_2$), 40.3 ($N(CH_3)_2$), 123.6 (CH), 124.1 (CH), 124.2 (CH), 142.7 (C-CH-$(Me)_2$), 142.8 (C-CH-$(Me)_2$), 144.3 (N-C), 168.4 (NCN).

*Synthesis of (**3c**).* In a dry Schlenk, tetrahydrofuran (20 mL) was added to lithium dimethylamide (0.36 g, 7.0 mmol). To this, *N,N′*-di-*tert*-butyl-carbodiimide (1.35 mL, 7.0 mmol) was added dropwise, and the reaction mixture left to stir for 2 h. The clear solution was then transferred via cannula to another Schlenk containing copper(I) chloride (0.69 g, 7.0 mmol) and allowed to react for 2 h, after which time the volatiles were removed under reduced pressure, and hexane (20 mL) was added to the resultant residue. This was left to stir for 15 min and then the volatiles were removed under reduced pressure. The process was repeated twice more to remove any residual tetrahydrofuran. Further hexane (20 mL) was added, and the slurry was filtered through Celite to remove any insoluble materials followed

dx.doi.org/10.1021/ic201602m | *Inorg. Chem.* 2012, 51, 246−257

Table 6. Crystallographic Data for the Complexes 1c, 1d, 2a, 2b, 2d[a], 3c and 4c

	1c	1d	2a	2b	2d[a]	3c	4c
empirical formula	$C_{44}H_{96}Li_4N_{12}$	$C_{54}H_{80}Li_2N_6$	$C_{18}H_{40}Cu_2N_6$	$C_{30}H_{56}Cu_2N_6$	$C_{54}H_{80}Cu_2N_6$	$C_{24}H_{54}Cu_3N_7$	$C_{22}H_{48}Cl_1Cu_3N_6$
formula weight	821.09	827.12	467.64	627.89	940.32	631.39	622.73
T/K	150(2)	150(2)	150(2)	150(2)	150(2)	150(2)	150(2)
crystal system	monoclinic	monoclinic	orthorhombic	triclinic	monoclinic	monoclinic	triclinic
space group	$C2/c$	$P2_1/n$	$C222_1$	$P\bar{1}$	$C2/c$	$P2_1/n$	$P\bar{1}$
a (Å)	16.0800(2)	13.1600(2)	11.3540(2)	10.4150(3)	43.1820(4)	13.6340(1)	10.215(2)
b (Å)	15.8510(2)	20.7540(2)	21.2909(6)	11.3900(3)	13.0740(2)	15.6710(2)	10.644(2)
c (Å)	22.4240(3)	38.1730(3)	9.9530(2)	16.0510(4)	31.9510(3)	14.8520(2)	14.732(3)
α (deg)				97.087(2)			103.876(2)
β (deg)	109.363(2)	92.730(2)		107.597(2)	117.080(2)	94.945(1)	107.091(2)
γ (deg)				112.555(2)			98.077(2)
V	5392.23(12)	10414.06(15)	2406.01(9)	1613.01(7)	16060.8(2)	3161.44(6)	1447.4(5)
Z	8	4	4	2	12	4	2
ρ_{calc} mg/m^{-3}	1.011	1.055	1.291	1.293	1.167	1.326	1.429
μ(Mo-K$_\alpha$), mm^{-1}	0.060	0.061	1.780	1.346	0.833	2.023	2.296
F(000)	1824	3616	992	672	6048	1336	652
crystal size, mm	0.25 × 0.20 × 0.15	0.32 × 0.20 × 0.20	0.20 × 0.17 × 0.15	0.22 × 0.10 × 0.08	0.20 × 0.15 × 0.10	0.40 × 0.25 × 0.10	0.25 × 0.25 × 0.10
θ range (deg)	8.53 to 28.27	4.44 to 27.47	3.59 to 27.49	3.10 to 28.25	8.52 to 27.10	3.25 to 28.29	8.17 to 27.44
reflections collected	44134	143043	14843	18809		66451	19713
independent reflections [R(int)]	6472 [0.1049]	23687 [0.0804]	2758 [0.0554]	7863 [0.0833]		7827 [0.0580]	6405 [0.0558]
reflections observed [$I > 2\sigma(I)$]	5297	14089	2548	4894		6516	5707
max., min transmission	0.9910, 0.9851	0.9879, 0.9808	0.7761, 0.7172	0.8999, 0.7561		0.8233, 0.4984	0.8029, 0.5975
goodness-of-fit	1.050	1.018	1.050	0.985		1.039	1.100
final $R1$ (wR_2) [$I > 2\sigma(I)$]	0.0451 (0.1181)	0.0575 (0.1214)	0.0309 (0.0746)	0.0479 (0.0945)		0.0291 (0.0659)	0.0308 (0.0758)
final $R1$ (wR_2) (all data)	0.0571 (0.1268)	0.1151 (0.1445)	0.0376 (0.0776)	0.1035 (0.1148)		0.0403 (0.0710)	0.0364 (0.0788)
Largest diff. peak and hole, e Å^{-3}	0.254 and −0.145	0.248 and −0.264	0.630 and −0.473	0.642 and −0.756		0.473 and −0.447	0.546 and −0.609

[a]Crystallographic data for the complex **2d** is reported here but has not been deposited with the CCDC.

by removal of the volatiles in vacuo. The resulting yellow crude product was purified by recrystallization from hexane −28 °C, to afford the final product as colorless crystals (1.10 g, 71% based on copper). Mp 97 °C (dec). Elemental analysis: calcd. for $C_{24}H_{56}Cu_3N_7$; C, 45.66, H, 8.62, N, 15.53, found: C, 44.65, H, 8.24, N, 15.53%. ^{1}H NMR (C_6D_6, 300.22 MHz) δ: 1.41 (s, 18H, NC(CH_3)$_3$), 1.48 (s, 18H, NC(CH_3)$_3$, 2.41 (s, 12H, CN(CH_3)$_2$, 3.09 (s, 6H, CuN(CH_3)$_2$). ^{13}C NMR (C_6D_6, 75.49 MHz) δ: 33.4 (NC($\underline{C}H_3$)$_3$), 34.7 (NC($\underline{C}H_3$)$_3$), 42.6 (CN($\underline{C}H_3$)$_2$), 49.3 (CuN($\underline{C}H_3$)$_2$), 54.4 (N$\underline{C}$(CH$_3$)$_3$), 55.9 (N$\underline{C}$(CH$_3$)$_3$), 168.3 (N$\underline{C}$N).

Synthesis of (4c). To a dry Schlenk, tetrahydrofuran (20 mL) was added to **1c** (0.82 g, 1.0 mmol) to give a colorless solution. The solution was then was then transferred via cannula to another Schlenk containing copper(I) chloride (0.59 g, 6.0 mmol) and allowed to react for 2 h, after which time the volatiles were removed under reduced pressure and dry hexane (20 mL) was added to the resultant residue. This was left to stir for 15 min and then the volatiles were removed under reduced pressure. The process was repeated twice more to remove any residual tetrahydrofuran. Further hexane (20 mL) was added, and the slurry was filtered through Celite to remove any insoluble materials followed by removal of the volatiles in vacuo. The resulting yellow crude product was purified by recrystallization from hexane, at −28 °C, to afford the product as colorless crystals (0.90 g, 72% based on copper). Mp 102 °C (dec). Elemental analysis: calcd. for $C_{22}H_{48}Cu_3N_6Cl$; C, 42.43, H, 7.77, N, 13.50, found. C, 42.74, H, 7.79, N, 13.26%. ^{1}H NMR (C_6D_6, 300.22 MHz) δ: 1.35 (s, 18H, NC(CH_3)$_3$), 1.40 (s, 18H, NC(CH_3)$_3$, 2.38 (s, 12H, CN(CH_3)$_2$. ^{13}C NMR (C_6D_6, 75.49 MHz) δ: 33.0 (NC($\underline{C}H_3$)$_3$), 34.4 (NC($\underline{C}H_3$)$_3$), 42.4 (CN($\underline{C}H_3$)$_2$), 54.4 (N$\underline{C}$(CH$_3$)$_3$), 55.7 (NC(CH$_3$)$_3$), 168.4 (N$\underline{C}$N).

Crystallography. Experimental details relating to the single-crystal X-ray crystallographic studies are summarized in Table 6. For all structures, data were collected on a Nonius Kappa CCD diffractometer at 150(2) K using Mo-Kα radiation (λ = 0.71073 Å). Structure solution and refinements were performed using SHELX86[31] and SHELX97[32] software, respectively. Corrections for absorption were made in all cases. For all complexes, hydrogen atoms were included at calculated positions.

■ ASSOCIATED CONTENT

Supporting Information

The X-ray crystallographic files in CIF format. This material is available free of charge via the Internet at http://pubs.acs.org.

■ AUTHOR INFORMATION

Corresponding Author

*E-mail: A.L.Johnson@bath.ac.uk. Phone: 44 (0)1225 384467. Fax: 44 (0)1225 386231.

■ ACKNOWLEDGMENTS

We acknowledge the financial support of the University of Bath and the EPSRC for the award of a CASE for New Academics (A.M.W.) and studentships to T.P.R. and T.P.

■ REFERENCES

(1) (a) Edelmann, F. T. *Adv. Organomet. Chem.* **2008**, *57*, 183−352. (b) Mohamed, A. A. *Coord. Chem. Rev.* **2010**, *254*, 1918−1947. (c) Schmidt, J. A. R.; Arnold, J. *J. Chem. Soc., Dalton Trans.* **2002**, 3454−3461. (d) Bailey, P. J.; Pace, S. *Coord. Chem. Rev.* **2001**, *214*, 91−141. (e) Bailey, P. J.; Grant, K. J.; Mitchell, L. A.; Pace, S.; Parkin, A.; Parsons, S. *J. Chem. Soc., Dalton Trans.* **2000**, 1887−1891.

(2) (a) Gordon, R. G.; Lim, B. S.; Rahtu, A.; Park, J. S. *Inorg. Chem.* **2003**, *42*, 7951−7958. (b) Jiang, X.; Bollinger, J. C.; Lee, D. *J. Am. Chem. Soc.* **2005**, *127*, 15678−15679. (c) Jiang, X.; Bollinger John, C.; Baik, M.-H.; Lee, D. *Chem. Commun.* **2005**, 1043−1045. (d) Li, Z.; Barry, S. T.; Gordon, R. G. *Inorg. Chem.* **2005**, *44*, 1728−1735. (e) Li, Z.; Rahtu, A.; Gordon, R. G. *J. Electrochem. Soc.* **2006**, *153*, C787−C794. (f) Chen, T.; Xu, C.; Baum, T. H.; Hendrix, B. C.; Cameron, T.; Roeder, J. F.; Stender, M.; Advanced Technology Materials, Inc., U.S.A. *U.S. Patent Appl. Publ.* WO-2007142700, 2006-US62709, 2007. (g) Coyle, J. P.; Monillas, W. H.; Yap, G. P. A.; Barry, S. T. *Inorg. Chem.* **2008**, *47*, 683−689. (h) Mohamed, A. A.; Abdou, H. E.; Mayer, A.; Fackler, J. P. Jr. *J. Cluster Sci.* **2008**, *19*, 551−559. (i) Bunge, S. D.; Steele, J. L. *Inorg. Chem.* **2009**, *48*, 2701−2706. (j) Johnson, A. L.; Willcocks, A. M.; Richards, S. P. *Inorg. Chem.* **2009**, *48*, 8613−8622. (k) Barry, S. T.; Whitehorne, T. J. J.; Coyle, J. P.; Mahmood, A.; Monillas, W. H.; Yap, G. P. A. *Eur. J. Inorg. Chem.* **2011**, 3240−3247. (l) Krisyuk, V.; Aloui, L.; Prud'homme, N.; Sysoev, S.; Senocq, F.; Samelor, D.; Vahlas, C. *Electrochem. Solid-State Lett.* **2011**, *14*, D26−D29.

(3) (a) Pyykko, P. *Chem. Rev.* **1997**, *97*, 597−636. (b) Pyykko, P.; Mendizabal, F. *Chem.—Eur. J.* **1997**, *3*, 1458−1465. (c) Pyykko, P.; Runeberg, N.; Mendizabal, F. *Chem.—Eur. J.* **1997**, *3*, 1451−1457.

(4) (a) Irwin Michael, D.; Abdou Hanan, E.; Mohamed Ahmed, A.; Fackler John, P. Jr. *Chem. Commun.* **2003**, 2882−2883. (b) Maier, S.; Hiller, W.; Straehle, J.; Ergezinger, C.; Dehnicke, K. *Z. Naturforsch., B: Chem. Sci.* **1988**, *43*, 1628−1632.

(5) Coyle, J. P.; Johnson, P. A.; DiLabio, G. A.; Barry, S. T.; Mueller, J. *Inorg. Chem.* **2010**, *49*, 2844−2850.

(6) Shibayama, K.; Seidel, S. W.; Novak, B. M. *Macromolecules* **1997**, *30*, 3159−3163.

(7) *Guanidines: Historical, Biological, Biochemical and Clinical Aspects of the Naturally Occurring Guanidino Compounds*; Mori, A., Cohen, B. D., Lowenthal, A., Eds.; Plenum Press: New york, 1985.

(8) (a) Cotton, F. A.; Feng, X. J.; Timmons, D. J. *Inorg. Chem.* **1998**, *37*, 4066−4069. (b) Oakley, S. H.; Coles, M. P.; Hitchcock, P. B. *Inorg. Chem.* **2004**, *43*, 5168−5170. (c) Oakley, S. H.; Soria, D. B.; Coles, M. P.; Hitchcock, P. B. *Dalton Trans.* **2004**, 537−546. (d) Oakley, S. H.; Coles, M. P.; Hitchcock, P. B. *Inorg. Chem.* **2003**, *42*, 3154−3156. (e) Coles, M. P.; Hitchcock, P. B. *Polyhedron* **2001**, *20*, 3027−3032.

(9) (a) Bunge, S. D.; Bertke, J. A.; Cleland, T. L. *Inorg. Chem.* **2009**, *48*, 8037−8043. (b) Bunge, S. D.; Ocana, J. A.; Cleland, T. L.; Steele, J. L. *Inorg. Chem.* **2009**, *48*, 4619−4621.

(10) Lim, B. S.; Rahtu, A.; Gordon, R. G. *Nat. Mater.* **2003**, *2*, 749−754.

(11) Li, Z. W.; Gordon, R. G.; Farmer, D. B.; Lin, Y. B.; Vlassak, J. *Electrochem. Solid-State Lett.* **2005**, *8*, G182−G185.

(12) Li, Z. W.; Gordon, R. G. *Chem. Vap. Deposition* **2006**, *12*, 435−441.

(13) Li, Z. W.; Rahtu, A.; Gordon, R. G. *J. Electrochem. Soc.* **2006**, *153*, C787−C794.

(14) Dai, M.; Kwon, J.; Halls, M. D.; Gordon, R. G.; Chabal, Y. J. *Langmuir* **2010**, *26*, 3911−3917.

(15) Ma, Q.; Guo, H. S.; Gordon, R. G.; Zaera, F. *Chem. Mater.* **2010**, *22*, 352−359.

(16) Bondi, A. *J. Phys. Chem.* **1964**, *68*, 441−451.

(17) (a) Fu, W. F.; Gan, X.; Che, C. M.; Cao, Q. Y.; Zhou, Z. Y.; Zhu, N. N. Y. *Chem.—Eur. J.* **2004**, *10*, 2228−2236. (b) Jakle, F.; Sundararaman, A.; Zakharov, L. N.; Rheingold, A. L. *Chem. Commun.* **2005**, 1708−1710. (c) Yin, Y. G.; Zhang, J. X.; He, J.; Hu, M. H.; Li, D.; Huang, X. C. *Inorg. Chem.* **2008**, *47*, 3471−3473. (d) Merz, K. M.; Hoffmann, R. *Inorg. Chem.* **1988**, *27*, 2120−2127.

(18) (a) Tsipis, C. A.; Karagiannis, E. E. *Organometallics* **2010**, *29*, 847−859. (b) Tsipis, A. C. *Organometallics* **2010**, *29*, 354−363. (c) Schwerdtfeger, P.; Assadollahzadeh, B. *Chem. Phys. Lett.* **2008**, *462*, 222−228. (d) Schwerdtfeger, P.; Hermann, H. L.; Boche, G. *Chem.—Eur. J.* **2001**, *7*, 5333−5342.

(19) (a) Siemeling, U.; Vorfeld, U.; Neumann, B.; Stammler, H. G. *Chem. Commun.* **1997**, 1723−1724. (b) Mendizabal, F.; Reyes, D.; Olea-Azar, C. *Int. J. Quantum Chem.* **2006**, *106*, 906−912.

(20) Kenney, A. P.; Yap, G. P. A.; Richeson, D. S.; Barry, S. T. *Inorg. Chem.* **2005**, *44*, 2926−2933.

(21) (a) Braga, D.; Grepioni, F.; Biradha, K.; Desiraju, G. R. *J. Chem. Soc., Dalton Trans.* **1996**, 3925−3930. (b) Jin, G. X.; Jones, C.; Junk, P. C.; Lippert, K. A.; Rose, R. P.; Stasch, A. *New J. Chem.* **2009**, *33*, 64−75.

(22) Cameron, T. M.; Xu, C. Y.; Dipasquale, A. G.; Rheingold, A. L. *Organometallics* **2008**, *27*, 1596−1604.

(23) Nikonov, G. I.; Shirobokov, O. G.; Gorelsky, S. I.; Simionescu, R.; Kuzmina, L. G. *Chem. Commun.* **2010**, *46*, 7831−7833.

(24) Woo, T. K.; Rowley, C. N.; Ong, T. G.; Priem, J.; Richeson, D. S. *Inorg. Chem.* **2008**, *47*, 9660−9668.

(25) Rowley, C. N.; DiLabio, G. A.; Barry, S. T. *Inorg. Chem.* **2005**, *44*, 1983−1991.

(26) Guo, D. L.; Qiao, X. L.; Tong, H. B.; Zhou, M. S. *Acta Crystallogr., Sect. E* **2009**, *65*, m405−u572.

(27) Gambarotta, S.; Bracci, M.; Floriani, C.; Chiesivilla, A.; Guastini, C. *J. Chem. Soc., Dalton Trans.* **1987**, 1883−1888.

(28) Kohn, R. D.; Pan, Z.; Mahon, M. F.; Kociok-Kohn, G. *Chem. Commun.* **2003**, 1272−1273.

(29) (a) Niemeyer, M. *Acta Crystallogr., Sect. E* **2001**, *57*, m491−m493. (b) Chen, H.; Olmstead, M. M.; Shoner, S. C.; Power, P. P. *J. Chem. Soc., Dalton Trans.* **1992**, 451−457.

(30) (a) Chivers, T.; Parvez, M.; Schatte, G. *J. Organomet. Chem.* **1998**, *550*, 213−220. (b) Coles, M. P.; Hitchcock, P. B. *Chem. Commun.* **2005**, 3165−3167. (c) Ong, T. G.; O'Brien, J. S.; Korobkov, I.; Richeson, D. S. *Organometallics* **2006**, *25*, 4728−4730. (d) Rudolf, D.; Kaifer, E.; Himmel, H. J. *Eur. J. Inorg. Chem.* **2010**, 4952−4961. (e) Schmidt, J. A. R.; Arnold, J. *Chem. Commun.* **1999**, 2149−2150.

(31) Sheldrick, G. M. *SHELX-86, Computer Program for Crystal Structure Determination*; University Of Göttingen: Göttingen, Germany, 1986.

(32) (a) Sheldrick, G. M. *SHELX-97, Computer Program for Crystal Structure Refinement*; Univerity of Göttingen: Göttingen, Germany, 1997; (b) Sheldrick, G. M. *Acta Crystallogr., Sect. A* **2008**, *64*, 112−122.